

CHARACTERIZATION OF SOME NEW ALKALI METAL MOLYBDATE HYDRATES BY THERMAL AND X-RAY METHODS

*N. L. Misra**, *K. D. Singh Mudher* and *V. Venugopal*

Fuel Chemistry Division, Bhabha Atomic Research Centre, Mumbai 400 085, India

(Received November 3, 2003; in revised form February 27, 2004)

Abstract

Preparation and characterization of four new hydrated alkali metal molybdates $\text{Na}_2\text{Mo}_4\text{O}_{13}\cdot 6\text{H}_2\text{O}$, $\text{K}_2\text{Mo}_4\text{O}_{13}\cdot 3\text{H}_2\text{O}$, $\text{Rb}_2\text{Mo}_4\text{O}_{13}\cdot 2\text{H}_2\text{O}$ and $\text{Cs}_2\text{Mo}_4\text{O}_{13}\cdot 2\text{H}_2\text{O}$ are described. The compounds were prepared by crystallizing the solution obtained by dissolving MoO_3 and corresponding alkali metal carbonates A_2CO_3 or molybdate A_2MoO_4 in stoichiometric amount in distilled water. The hydrated molybdates were characterized by thermal (TG/DTA) and X-ray diffraction (XRD) methods. The number of water molecules in the compounds were determined from their TG /DTA curves recorded in air and identification of their dehydration products was done by XRD. The cell parameters of the compounds were obtained by indexing their XRD patterns. Attempt to prepare the corresponding hydrated compound of lithium was not successful.

Keywords: alkali metals, molybdates, thermal analysis (TG/DTA), X-ray diffraction (XRD)

Introduction

Molybdenum is an important fission product formed during the fission of ^{235}U or ^{239}Pu based fuels in a nuclear reactor and is also a constituent of stainless steel cladding material used in fast reactors. Different molybdates are formed during the interaction of molybdenum with other fission products, nuclear fuel, constituents of cladding materials [1–4] and during reprocessing of spent nuclear fuel. Molybdates also find their application as anticorrosive materials, catalyst in oxidation of organic substances and as inorganic ion exchangers [9–17]. Recently, alkali metal molybdates have been studied for their use as catalyst for the partial oxidation of methane [15]. Alkali metals Cs and Rb are important fission products formed in the reactor in large yield and Na is a coolant for fast breeder reactors [2]. Hence alkali metal molybdates have a special relevance in nuclear fuel cycle.

Though the preparation and characterization of anhydrous alkali metal molybdates are reported in [18–21], studies on hydrated alkali metal molybdates are limited [22–24].

* Author for correspondence: E-mail: nlmisra@magnum.barc.ernet.in

A systematic study was carried out on the preparation and characterization of new alkali metal hydrated molybdates of general formula $A_2Mo_4O_{13} \cdot xH_2O$ (where A =alkali metals and x =number of water molecules) with an aim to investigate the reduction of the corresponding anhydrous molybdates $A_2Mo_4O_{13}$ to mixed valent molybdates $A_2Mo_4O_{12}$ in similar way as reported for the corresponding uranates [25].

Experimental

Preparation

All chemicals used were of A.R. grade. Weighed amounts of A_2MoO_4 or A_2CO_3 (A =Na, K, Rb and Cs) were dissolved in distilled water and the resultant solutions were heated slowly till boiling on a hot plate. Required amount of MoO_3 to give $A:Mo$ atomic ratio of 1:2 was added slowly to the boiling solution with constant stirring. The resultant solution was filtered and the filtrate was kept under an IR lamp and evaporated slowly to crystallize white coloured hydrated molybdates of Na and light yellow coloured hydrated molybdates of K, Rb and Cs. While crystallization was very easy in case of cesium and rubidium, crystallization of the corresponding sodium and potassium compounds could be achieved with diluted solutions only. The lithium-hydrated molybdates $Li_2Mo_4O_{13} \cdot xH_2O$ could not be prepared even after several attempts following the above procedure. The filtrate obtained by dissolving MoO_3 in dilute boiling solution of Li_2CO_3 turned to a blue coloured syrupy liquid when kept under the IR lamp and crystallization was not possible.

Characterization

The compounds formed were characterized by thermal (TG/DTA) and X-ray powder diffraction (XRD) methods. Simultaneous TG and DTA curves of the compounds taken in platinum cups were recorded in an ULVAC thermal analyzer in flow of Zero-air comprising 78% N_2 and 22% O_2 with a heating rate of $5^\circ C \text{ min}^{-1}$. However, to differentiate some overlapping TG mass loss steps slower heating rates up to $2^\circ C \text{ min}^{-1}$ were also used. Preheated alumina was used as a standard reference material for DTA. Mass sensitivity for the TG balance was 0.1 mg. The temperature and mass calibration of the instrument is carried out in different temperature ranges and ambient using ICTAC standards routinely. The free moisture in samples, if any, was removed initially by recording the thermal pattern in isothermal conditions at room temperature for about 30 min to obtain a straight base line in TG curves. XRD patterns of the compounds were recorded on a DIANO X-ray powder diffractometer using monochromatized CuK_α radiation ($\lambda=1.5405 \text{ \AA}$). The powder samples for XRD were ground with 10% solution of collodion in iso-amyl acetate and a thin film of the mull, thus obtained, was made on a glass slide. The thin coating of collodion protects the samples from absorbing moisture. This slide was presented for XRD analysis immediately after drying in hot air. The number of water molecules in the compounds was determined from their TG/DTA curves and XRD patterns of the heated product.

Results and discussion

$\text{Na}_2\text{Mo}_4\text{O}_{13}\cdot 6\text{H}_2\text{O}$

The TG and DTA curves of $\text{Na}_2\text{Mo}_4\text{O}_{13}\cdot 6\text{H}_2\text{O}$ are shown in Fig. 1. TG shows mass loss in four steps in the range of 40–120, 140–180, 200–215 and 215–255°C accompanied by endothermic DTA peaks. The XRD pattern of the dehydration product obtained by heating the crystals at 420°C was similar to the reported XRD pattern of $\text{Na}_2\text{Mo}_4\text{O}_{13}$ [19]. Observed total mass loss of 14.40% corresponds to mass loss of 6 water molecules (Expected mass loss=14.48%). The stepwise mass loss indicated the number of water molecules lost in these steps to be 3, 2, 1/2 and 1/2, respectively. On controlled cooling at a rate of $10^\circ\text{C min}^{-1}$ after dehydration, no DTA peak was observed confirming that DTA peaks are due to dehydration. When the anhydrous $\text{Na}_2\text{Mo}_4\text{O}_{13}$ was further heated, it melted at 520°C, giving an endothermic DTA peak. Melting was confirmed by physical verification of the sample.

Powder XRD pattern of the hydrated crystals did not match with any of the reported phases of Na–Mo–O system. Hence it was concluded that the compound was new. On the basis of the mass loss shown by TG and XRD pattern of the end product, the chemical formula of the compound formed could be given as $\text{Na}_2\text{Mo}_4\text{O}_{13}\cdot 6\text{H}_2\text{O}$. The XRD pattern could be indexed on a monoclinic cell. The room temperature XRD pattern of the compound $\text{Na}_2\text{Mo}_4\text{O}_{13}\cdot 6\text{H}_2\text{O}$ (A) and of the products obtained by heating it up to 350°C (B), 420°C (C) are different. The XRD patterns reveal that (B) is an amorphous phase whereas (C) is a crystalline one. XRD pattern (C) was similar to the XRD pattern of the compound $\text{Na}_2\text{Mo}_4\text{O}_{13}$ reported in [19]. This indicates that after dehydration the compound changes to an amorphous phase, which becomes a crystalline phase on further heating. However no DTA peak corresponding to this crystallization was observed after dehydration while heating, indicating that the crystallization is either too slow or the heat of crystallization is too low to give a sharp DTA peak. The intermediate dehydration products could not be

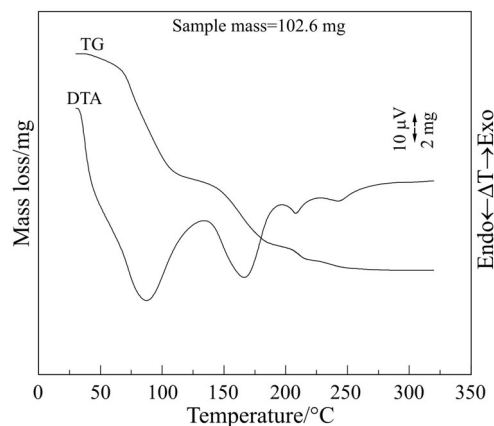


Fig. 1 TG and DTA curves of $\text{Na}_2\text{Mo}_4\text{O}_{13}\cdot 6\text{H}_2\text{O}$

isolated probably due to close proximity of temperatures at which water molecules are lost in different steps. The thermal behaviour of the compound, cell parameters and X-ray data are summarized in Tables 1, 2 and 3, respectively.

$K_2Mo_4O_{13} \cdot 3H_2O$

The TG and DTA curves of the $K_2Mo_4O_{13} \cdot 3H_2O$ are shown in Fig. 2. TG indicated mass loss in two steps in the temperature range of 40–100 and 150–185°C accompanied by two endothermic DTA peaks. On further heating an exothermic DTA peak at 260°C was observed without any mass change shown by TG. On controlled cooling from 320°C, no DTA peak could be observed. The XRD pattern of dehydrated product of $K_2Mo_4O_{13} \cdot 3H_2O$ obtained by heating it at 225°C is like that of an amorphous phase and of that obtained by heating at 400°C matched with the reported $K_2Mo_4O_{13}$ [20]. It is concluded that the first two endothermic DTA peaks are due to loss of water of hydration, whereas the exothermic DTA peak at 260°C is due to crystallization of the amorphous dehydration product formed. Total mass loss of 7.07% corresponds to three hydrated water molecules present in the compound (theoretical mass loss=7.46%). The stepwise mass loss shown by TG matched with two and one water molecules, respectively. On the basis of the mass loss and the XRD pattern of the crystalline dehydration product of the crystals, the composition of the initial hydrated compound could be given as $K_2Mo_4O_{13} \cdot 3H_2O$. Preparation of this compound and X-ray data are not reported in the literature. The thermal behaviour of the compound is summarized in Table 1. The anhydrous phase, $K_2Mo_4O_{13}$ on further heating melted at 540°C. The XRD pattern of dehydration product obtained by heating $K_2Mo_4O_{13} \cdot 3H_2O$ at 120°C for two hours was different from the starting compound and anhydrous $K_2Mo_4O_{13}$. On the basis of the mass loss shown in first step in the TG curve of $K_2Mo_4O_{13} \cdot 3H_2O$, this phase was characterized as $K_2Mo_4O_{13} \cdot H_2O$. On further heating this phase loses the remaining water molecules at 150–185°C. However XRD pattern of monohydrate was weak and could not be indexed. The XRD pattern of $K_2Mo_4O_{13} \cdot 3H_2O$ could be indexed on the basis of

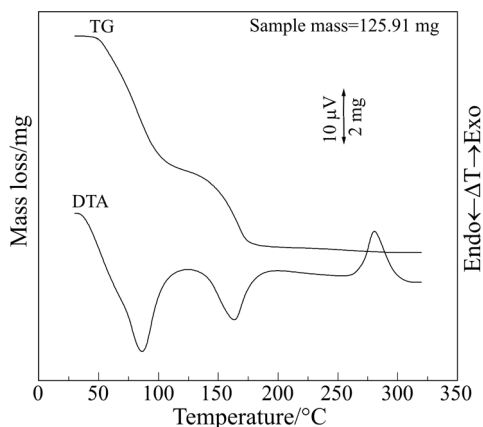


Fig. 2 TG and DTA curves of $K_2Mo_4O_{13} \cdot 3H_2O$

Table 1 Thermal behaviour of alkali metal molybdate hydrates

Compounds	Number of steps for loss of water molecules	Temperature range of successive water loss steps/°C	Number of water molecules lost in successive steps	Mass loss% due to loss of hydrated water molecules		Temperature of crystallization of corresponding anhydrous phase/°C
				Expected	As shown by TG	
$\text{Na}_2\text{Mo}_4\text{O}_{13} \cdot 6\text{H}_2\text{O}$	4	40–120, 140–180, 200–215, 215–255	3, 2, 1/2, 1/2	14.48	14.40	Not observed
$\text{K}_2\text{Mo}_4\text{O}_{13} \cdot 3\text{H}_2\text{O}$	2	40–100, 150–185	2, 1	7.46	7.07	260
$\text{Rb}_2\text{Mo}_4\text{O}_{13} \cdot 2\text{H}_2\text{O}$	1	60–140	2	4.51	4.37	280
$\text{Cs}_2\text{Mo}_4\text{O}_{13} \cdot 2\text{H}_2\text{O}$	1	50–130	2	4.03	3.47	280

orthorhombic cell and the cell parameters are tabulated in Table 2. The X-ray data on $K_2Mo_4O_{13} \cdot 3H_2O$ are given in Table 3.

Table 2 Cell parameters of different hydrated alkali metal molybdates

Compounds	Crystal system	Cell parameters (a, b, c in Å, α, β, γ in degrees)
$Na_2Mo_4O_{13} \cdot 6H_2O$	monoclinic	$a=10.825(4)$, $b=14.509(5)$, $c=8.194(3)$, $\beta=98.15(5)$
$K_2Mo_4O_{13} \cdot 3H_2O$	orthorhombic	$a=13.310(5)$, $b=9.522(5)$, $c=13.400(9)$
$Rb_2Mo_4O_{13} \cdot 2H_2O$	orthorhombic	$a=16.720(7)$, $b=19.313(9)$, $c=5.404(2)$
$Cs_2Mo_4O_{13} \cdot 2H_2O$	monoclinic	$a=15.403(9)$, $b=12.909(6)$, $c=9.928(7)$, $\beta=97.72(5)$

Rb₂Mo₄O₁₃·2H₂O and Cs₂Mo₄O₁₃·2H₂O

The light yellow coloured crystals of $Rb_2Mo_4O_{13} \cdot 2H_2O$ gave TG and DTA curves as shown in Fig. 3. TG showed a mass loss in single step in the temperature range of 60–140°C accompanied by an endothermic DTA peak. On further heating DTA showed an exothermic peak at 280°C. The XRD pattern of the initial compound at room temperature, that heated up to 150 and 350°C were different. XRD pattern of the product heated up to 150°C was like that of an amorphous material. The XRD pattern of the end product obtained after heating $Rb_2Mo_4O_{13} \cdot 2H_2O$ up to 350°C was similar to the XRD pattern of the compound $Rb_2Mo_4O_{13}$ reported in [20]. Single step mass loss shown by TG was equivalent to two water molecules (observed mass loss shown by TG was 4.36% compared to theoretical mass loss of 4.51%). On controlled cooling from 400°C no DTA peak was observed. This gives an inference that the endothermic DTA peak obtained while heating the sample is due to water loss whereas the exothermic DTA peak is due to crystallization of the anhydrous amorphous phase formed after dehydration of

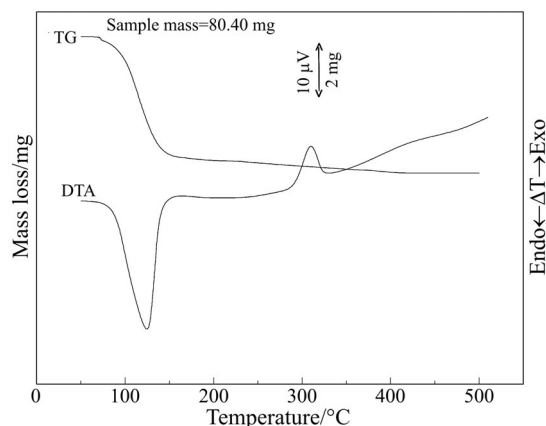


Fig. 3 TG and DTA curves of $Rb_2Mo_4O_{13} \cdot 2H_2O$

Table 3 X-ray data on $\text{Na}_2\text{Mo}_4\text{O}_{13}\cdot 6\text{H}_2\text{O}$ and $\text{K}_2\text{Mo}_4\text{O}_{13}\cdot 3\text{H}_2\text{O}$

<i>h k l</i>	$\text{Na}_2\text{Mo}_4\text{O}_{13}\cdot 6\text{H}_2\text{O}$		Relative intensity <i>I/I</i> ₀	<i>h k l</i>	$\text{K}_2\text{Mo}_4\text{O}_{13}\cdot 3\text{H}_2\text{O}$		Relative intensity <i>I/I</i> ₀
	<i>d</i> _{obs} /Å	<i>d</i> _{calc} /Å			<i>d</i> _{obs} /Å	<i>d</i> _{calc} /Å	
1 0 0	10.67	1.072	30	0 1 0	9.50	9.52	100
0 0 1	8.07	8.11	21	1 1 0	7.72	7.74	94
-1 0 1	6.96	6.96	100	2 0 0	6.66	6.66	11
-1 1 1	6.29	6.28	5	2 1 0	5.43	5.46	9
1 2 0	6.01	6.01	7	1 2 0	4.47	4.48	4
1 1 1	5.59	5.60	11	0 2 2	3.90	3.88	14
2 1 0	5.03	5.03	6	2 2 1	3.72	3.72	21
-2 0 1	4.80	4.79	8	2 2 2	3.35	3.35	21
-1 2 1	4.65	4.65	8	0 3 0	3.18	3.17	62
2 0 1	4.21	4.21	11	1 3 0	3.09	3.09	19
0 1 2	3.91	3.91	8	2 3 1	2.801	2.802	12
1 3 4	3.78	3.78	8	0 2 4	2.735	2.740	5
0 4 0	3.63	3.63	8	5 0 0	2.660	2.662	5
3 1 0	3.47	3.47	14	5 0 1	2.608	2.611	5
0 4 1	3.31	3.31	8	5 0 2	2.478	2.474	5
2 3 1	3.17	3.17	15	5 1 2	2.393	2.394	8
-1 3 2	3.07	3.08	13	4 0 4	2.359	2.361	20
2 0 2	3.03	3.03	9	5 2 0	2.323	2.323	6
3 3 0	2.871	2.873	9	4 3 1	2.265	2.264	20
-1 1 3	2.669	2.668	5	0 4 3	2.100	2.101	29
-1 2 3	2.541	2.542	7	1 3 5	2.024	2.024	13
4 2 1	2.315	2.315	5	7 0 1	1.883	1.883	9
2 2 3	2.182	2.181	7	0 4 5	1.779	1.780	3
0 0 4	2.029	2.028	4	3 1 7	1.729	1.728	3
0 3 4	1.870	1.870	4	8 2 0	1.571	1.571	9
2 6 2	1.893	1.891	3				
6 2 0	1.735	1.734	6				
6 3 0	1.675	1.675	6				
-2 8 2	1.609	1.608	4				

*d*_{obs}: Experimentally measured *d*-spacing, *d*_{cal}: calculated *d*-spacing from *h, k, l*

$\text{Rb}_2\text{Mo}_4\text{O}_{13}\cdot 2\text{H}_2\text{O}$. On further heating it was found that the anhydrous compound melted at 540°C. The XRD pattern of the initial hydrated compound was not matching with any

of the compounds of rubidium and molybdenum reported in literature. On the basis of the TG, DTA curves and XRD pattern of the end product it can be concluded that the initial compound is a new compound and it can be given chemical formula $\text{Rb}_2\text{Mo}_4\text{O}_{13}\cdot 2\text{H}_2\text{O}$. It loses water in single step (showing mass loss in TG and endothermic peak in DTA) and forms amorphous compound $\text{Rb}_2\text{Mo}_4\text{O}_{13}$. On further heating it crystallizes giving an exothermic DTA peak and no mass change shown by TG. Thermal behaviour of the compound is summarized in Table 1. The X-ray data on the new compound could be indexed on an orthorhombic cell and the cell parameters are given in Table 2. The X-ray data on the compound $\text{Rb}_2\text{Mo}_4\text{O}_{13}\cdot 2\text{H}_2\text{O}$ are given in Table 4.

The TG and DTA curves of $\text{Cs}_2\text{Mo}_4\text{O}_{13}\cdot 2\text{H}_2\text{O}$ in air are shown in Fig. 4. TG shows mass loss in a single step in the temperature range of 50–130°C. This mass loss is accompanied by an endothermic DTA peak. On further heating an exothermic peak at 280°C without any mass change shown by TG was observed. The XRD pattern of the initial compound at room temperature (A), after heating up to 150°C (B) and after heating up to 350°C (C) shows that these are completely different. The XRD pattern indicates that the product in case A is crystalline, in case B it is amorphous. The XRD pattern in case C was similar to the β -phase of the $\text{Cs}_2\text{Mo}_4\text{O}_{13}$ [21]. The total mass loss of 3.47% up to 400°C corresponds to two water molecules (Theoretical mass loss=4.03%). On the basis of thermal behaviour of hydrated compound and XRD pattern of the end product, the hydrated compound was characterized as $\text{Cs}_2\text{Mo}_4\text{O}_{13}\cdot 2\text{H}_2\text{O}$ and its X-ray diffraction pattern could be indexed on a monoclinic cell. When the anhydrous compound $\text{Cs}_2\text{Mo}_4\text{O}_{13}$ was further heated, it melted at 520°C. Thermal behaviour of the compound $\text{Cs}_2\text{Mo}_4\text{O}_{13}\cdot 2\text{H}_2\text{O}$, its cell parameters and X-ray data are summarized in Tables 1, 2 and 4, respectively.

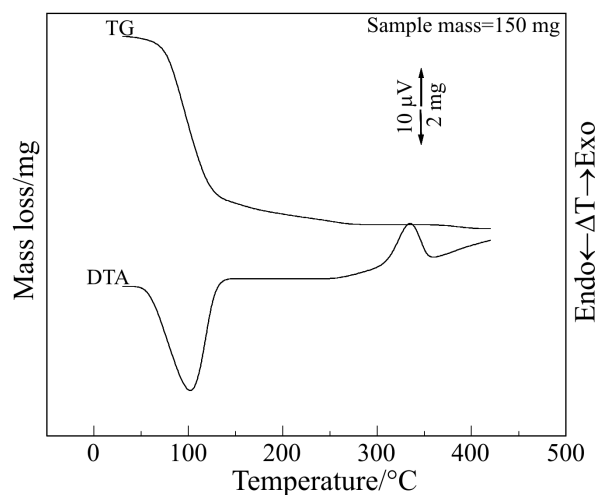


Fig. 4 TG and DTA curves of $\text{Cs}_2\text{Mo}_4\text{O}_{13}\cdot 2\text{H}_2\text{O}$

Table 4 X-ray data on $\text{Rb}_2\text{Mo}_4\text{O}_{13}\cdot 2\text{H}_2\text{O}$ and $\text{Cs}_2\text{Mo}_4\text{O}_{13}\cdot 2\text{H}_2\text{O}$

<i>h k l</i>	$\text{Rb}_2\text{Mo}_4\text{O}_{13}\cdot 2\text{H}_2\text{O}$		Relative intensity I/I_0	<i>h k l</i>	$\text{Cs}_2\text{Mo}_4\text{O}_{13}\cdot 2\text{H}_2\text{O}$		Relative intensity I/I_0
	$d_{\text{obs}}/\text{\AA}$	$d_{\text{calc}}/\text{\AA}$			$d_{\text{obs}}/\text{\AA}$	$d_{\text{calc}}/\text{\AA}$	
0 2 0	9.62	9.66	100	1 1 0	9.87	9.86	42
2 1 0	7.66	7.67	75	-1 0 1	8.86	8.83	4
2 2 0	6.32	6.32	4	1 0 1	7.80	7.81	100
3 0 0	5.59	5.57	3	-1 1 1	7.30	7.29	12
3 1 0	5.37	5.36	4	-2 0 1	6.50	6.47	9
1 3 1	4.02	4.02	7	0 2 1	5.40	5.40	15
3 1 1	3.81	3.80	24	1 3 0	4.15	4.14	11
2 3 1	3.71	3.71	2	-1 2 2	3.89	3.89	87
5 0 0	3.35	3.34	16	-4 0 1	3.73	3.73	30
3 5 0	3.17	3.18	62	-2 2 2	3.64	3.64	24
1 5 1	3.09	3.09	10	2 3 1	3.43	3.43	25
0 6 1	2.769	2.765	7	2 2 2	3.34	3.34	36
1 0 2	2.666	2.667	4	-3 2 2	3.28	3.28	42
6 3 0	2.555	2.557	2	1 4 0	3.16	3.16	17
0 7 1	2.460	2.457	3	0 2 3	2.923	2.924	15
6 4 0	2.413	2.414	10	4 0 2	2.839	2.836	9
2 3 2	2.384	2.388	3	-1 5 1	2.477	2.478	8
5 5 1	2.293	2.290	3	6 2 0	2.366	2.367	13
4 1 2	2.254	2.254	1	6 2 1	2.238	2.238	6
7 1 1	2.170	2.171	25	5 0 3	2.099	2.098	8
4 7 1	2.119	2.118	3	1 6 2	1.942	1.942	6
6 5 1	2.084	2.085	3	6 1 3	1.870	1.871	7
3 9 1	1.877	1.878	14				
5 5 2	1.846	1.846	3				
1 2 3	1.762	1.761	3				

d_{obs} : Experimentally measured d -spacing, d_{cal} : calculated d -spacing from h, k, l

Conclusions

From the thermal and X-ray studies of the hydrated and anhydrous compounds prepared in the present study it can be concluded that the compounds $\text{Na}_2\text{Mo}_4\text{O}_{13}\cdot 6\text{H}_2\text{O}$, $\text{K}_2\text{Mo}_4\text{O}_{13}\cdot 3\text{H}_2\text{O}$, $\text{Rb}_2\text{Mo}_4\text{O}_{13}\cdot 2\text{H}_2\text{O}$ and $\text{Cs}_2\text{Mo}_4\text{O}_{13}\cdot 2\text{H}_2\text{O}$ are new compounds and their cell parameters are reported in Table 2. These hydrated molybdates lose water of hydration to form anhydrous amorphous phase $\text{A}_2\text{Mo}_4\text{O}_{13}$. On further heating this amorphous phase crystallizes and finally melts. As the atomic

number of the alkali metals increases the number of water molecules in the corresponding hydrated molybdate $A_2Mo_4O_{13} \cdot xH_2O$ decreases and its preparation becomes easier.

* * *

The authors express their sincere thanks to Shri R. Prasad, Head, Fuel Development Chemistry Section, for his keen interest in the work.

References

- 1 H. Kleykamp, Nucl. Technol., 80 (1988) 416.
- 2 T. B. Lindemer, T. M. Besmann and C. E. Johnson, J. Nucl. Mater., 100 (1988) 178.
- 3 T. Ishii and T. Mizuno, J. Nucl. Mater., 231 (1996) 242.
- 4 M. Tourasse, M. Boidron and P. Pasquet, J. Nucl. Mater., 188 (1992) 49.
- 5 E. C. Buck, D. J. Wronkiewicz, P. A. Finn and J. K. Bates, J. Nucl. Mater., 249 (1997) 70.
- 6 O. A. Ustinov, IAEA Report no. IAEA-SM-358 (1999) on Reprocessing of mixed U-Pu Fuel by recrystallization in molten molybdates.
- 7 J. S. Kim, B. C. Song, K. Y. Jee, J. G. Kim and K. S. Chun, J. Korean Nucl. Soc., 30 (1998) 99.
- 8 B. S. M. Rao, E. Gantner, J. Reinhardt, D. Steinert and H. J. Ache, J. Nucl. Mater., 170 (1990) 39.
- 9 V. Moutarlier, M. P. Gigandet, J. Pagetti and B. Normand, Surf. Coat. Technol., 161 (2002) 267.
- 10 V. Moutarlier, M. P. Gigandet, L. Ricq and J. Pagetty, Appl. Surf. Sci., 183 (2001) 1.
- 11 K. Aramaki, Corros. Sci., 433 (2001) 59.
- 12 L. M. Madeira, J. M. Herrmann, J. Disdier, M. F. Portela and F. G. Freire, Appl. Catal. A, 235 (2002) 1.
- 13 M. Kurzawa and D. Dabrowska, J. Therm. Anal. Cal., 60 (2000) 183.
- 14 N. R. E. Radwan, M. Mokhtar and G. A. El-Shobaky, J. Therm. Anal. Cal., 71 (2003) 977.
- 15 A. Erdöhelyi, K. Fodor, R. Németh, A. Hancz and A. Oszko, J. Catal., 199 (2001) 328.
- 16 J. B. Black, N. J. Clayden, P. L. Gai, J. D. Scott, E. M. Serwicka and J. B. Goodenough, J. Catal., 106 (1987) 1.
- 17 U. N. Choube, B. V. Labdhe and Z. R. Turel, Proc. Nuclear and Radiochemistry Symposium Febr. 7–10, 2001, Pune, India.
- 18 A. K. Ganguli, L. Ganapathi, J. Gopalakrishnan and C. N. R. Rao, J. Solid State Chem., 74 (1988) 228.
- 19 V. A. Balashov and A. A. Majer, Russ. J. Inorg. Mater Eng. Transl., 6 (1970) 1276.
- 20 B. M. Gatehouse and P. Leverett, J. Chem. Soc., A (1971) 2107.
- 21 N. L. Misra, K. L. Chawla, V. Venugopal and D. D. Sood, J. Alloys and Comp., 284 (1999) 112.
- 22 K. Eda, S. Fukiharu, T. Suzuki and N. Sotani, J. Solid State Chem., 164 (2002) 157.
- 23 W. Surga, S. Sagnowski and S. Hodorowicz, J. Inorg. Nucl. Chem., 43 (1981) 1821.
- 24 W. Surga, J. Czerwonka and S. Hodorowicz, J. Thermal Anal., 21 (1981) 375.
- 25 K. L. Chawla, N. L. Misra and N. C. Jayadevan J. Nucl. Mater., 154 (1988) 181.